Clustering in rapid granular flows of binary and continuous particle size distributions

R. Brent Rice and Christine M. Hrenya*

Department of Chemical and Biological Engineering, University of Colorado, Boulder, Colorado 80309, USA

(Received 29 April 2009; revised manuscript received 10 January 2010; published 8 February 2010)

The dynamic clustering phenomenon in two-dimensional simple shear flows has been investigated using molecular dynamic simulations of systems containing binary and continuous size distributions of equal-material-density particles. Particular attention has been paid to two questions: (1) Does the presence of size nonuniformities serve to enhance or attenuate the presence of clusters? (2) Do particles of a given size preferentially segregate within the clusters? With respect to the first question, the prominence of clustered regions increases with increasing deviation from the monodisperse limit in the case of both binary and continuous size distributions. With respect to the second question, the larger particles of both binary and continuous size distributions are consistently observed to segregate within the *transient* clustered regions. Further investigation of granular temperatures within the clustered and dilute regions reveals that this segregation is consistent with previously observed temperature-driven segregation in *steady-state* systems; large particles favor the lower-temperature (clustered) regions. Moreover, observation of clustering length scales suggests that large particles may favor the center of the clustered regions, where granular temperatures are expected to reach a minimum.

DOI: 10.1103/PhysRevE.81.021302 PACS number(s): 45.70.Qj, 47.11.Mn

I. INTRODUCTION

The coffee that we grind each morning and the sandy beaches on which we run each summer serve as simple reminders of the impact of granular materials on our daily lives. Industrial settings further reflect our dependence on these materials by the fact that both raw materials and final products are often solid in form [1]. In spite of this prevalence, the understanding of systems containing granular materials is limited [2–6]. Inhomogeneities in the spatial distribution of particles (clusters) and de-mixing (in mixtures of unlike particles) are a few of the ill-understood phenomena that arise. From the perspective of the pharmaceutical, agricultural, mining, and chemical industries, such lack of predictive understanding translates into significant losses and inefficiencies. For example, it is not uncommon for solids-handling operations to run at 40%–50% of their design capacity [7]. It follows that the study of granular materials and their behavior is crucial to the improvement of design and efficiency. Accordingly, the current effort aims to further insight regarding two ill-understood phenomena noted above: clustering and segregation (de-mixing) within mixtures of unlike particles. More specifically, the nature of dynamic clusters in simple shear flow systems is studied with respect to the effect of multiple particle sizes, and attention is directed to rapid granular flows.

Hopkins and Louge [8] reported early molecular dynamics (MD) observations of dynamic clusters for systems under simple shear, where clusters were observed to be most prominent at moderate particle concentrations and low restitution coefficients. Clustering has since been well established in MD simulations of a variety of idealized granular systems (e.g., homogeneous cooling systems [9–11], simple shear systems [12–14], and Couette systems [15,16]), though the form of the density inhomogeneities may depend on the system in which they appear. Practically, the importance of clusters has been noted for such varied systems as planetary rings [17–19], high-velocity fluidized beds [20–22], and granular jets [23].

While the majority of MD investigations pertaining to clusters have focused on monodisperse systems, the presence of clusters has been shown to persist in systems containing multiple particle sizes. Alam and Luding [24] made a series of observations regarding clusters in binary systems under simple shear flow. Consistent with the monodisperse observations of Tan and Goldhirsch [12], the life cycle of these clusters consisted of rotation with time, stretching along an angle of 45° from the direction of shear, and collision with each other to form new clusters. Cluster sizes were found to vary. Moreover, a mass disparity between species of a binary (in size) mixture was shown to increase average and maximum cluster sizes compared to the same binary mixture in which both species had the same mass (i.e., the two species had different densities). For a Couette geometry, Conway and Glasser [16] considered a system of equally sized particles that were mildly polydisperse with respect to material density (and mass), and noted that the standing wave cluster formations persist in the polydisperse system, similar to the monodisperse counterparts. Later, Conway *et al.* [15] considered a Couette system containing a continuous size distribution. In addition to the persistence of clusters within these systems, the distribution of particle sizes was shown to vary strongly along the length of the standing wave. This nonhomogeneous distribution of particle species hints at the next key issue pertaining to polydisperse systems, namely, species segregation.

The issue of species segregation (and mixing) within granular systems is wrapped with great practical significance. For example, the inappropriate (or inconsistent) blending of active and inactive ingredients in a pharmaceutical product could render the product poisonous or ineffective rather than

*Author to whom correspondence should be addressed. hrenya@colorado.edu

beneficial. Accordingly, much research has been devoted to the understanding of prominent driving forces and mechanisms by which species segregate.

For rapid flows of unlike particles, one prominent feature of species segregation in *steady* flows is the association of more massive particles with the low-granular-temperature regions. Hsiau and Hunt [25] employed the kinetic theory of Jenkins and Mancini [26] to the study of oscillatory no-flow systems of elastic particles and sheared systems of inelastic particles, both of which exhibited steady-state temperature gradients. In both cases, predictions indicated that more massive particles favored the cooler regions. Later, binary mixtures with respect to size (and mass) were shown to exhibit similar segregation trends for zero-mean-flow systems bounded by thermal reservoirs [27], a moving bumpy boundary [28], and two walls of different temperature [29]. Furthermore, MD simulations of continuous particle size distributions bordered by two walls of different temperature revealed that the larger particles of the distribution also favored the cooler regions [30].

In addition to the temperature-gradient driving force noted above, several other driving forces associated with species segregation have been identified via an analysis of kinetic-theory-based equations, including concentration gradients, pressure gradients, external forces, and gradients in species temperature [29,31–34]. Such equations have been used by numerous researchers to predict segregation patterns in steady granular flows (i.e., systems without clustering instabilities) [35–41].

In comparison, few studies exist on species segregation in systems which exhibit clustering instabilities. Conway *et al.* [15] examined various types of binary mixtures in Couette flows with a plug instability. Comparisons of MD simulations (with clusters) with kinetic-theory-based prediction for one-dimensional *steady-state* flows (assuming no clustering) are favorable with the exception of a segregation reversal observed for equal-density mixtures. In a homogeneous cooling system, Cattuto and Marconi [10] reported segregation of the more massive particles of an equal-sized mixture toward the clustered regions. The explanation for this segregation relied not on gradients within the system, but on a particle mobility argument. The energy exchange between the light and heavy species was stated to result in the "effective repulsion of the light particles by the heavy particles," whereby small particles were able to more easily escape the clustered regions.

In the current work, the effect of both binary and continuous size distributions on the dynamic clusters observed in two-dimensional (2D) simple shear flow is investigated. For both size distributions, two primary questions are addressed: Does the presence of size nonuniformities serve to enhance or attenuate the presence of clusters? Do particles of a given size preferentially segregate within the clusters? Additionally, a potential driving force for the observed segregation, namely the presence of a granular temperature gradient, is explored.

II. COMPUTATIONAL APPROACH

The current study investigates clustering in two-dimensional, simple shear flow of polydisperse systems via MD simulations. Simple shear is achieved by Lees-Edwards boundary conditions. Due to a lack of body forces, the particles move along linear trajectories according to an event-driven algorithm [42]. Particles are treated as frictionless, inelastic, circular disks of constant material density, and collisions are resolved via a hard-sphere model [42],

$$\vec{v}_i^* = \vec{v}_i - \frac{m_j}{m_i + m_j}(1+e)(\vec{k}_{ij}\cdot\vec{v}_{ij})\vec{k}_{ij}, \tag{1}$$

$$\vec{v}_j^* = \vec{v}_j + \frac{m_i}{m_i + m_j}(1+e)(\vec{k}_{ij}\cdot\vec{v}_{ij})\vec{k}_{ij}, \tag{2}$$

where $\vec{v}$ is the velocity of a particle (i or j), $\vec{v}_{ij}$ is the relative velocity defined as $\vec{v}_j - \vec{v}_i$, $\vec{k}_{ij}$ is the unit vector pointing from the center of particle i to the center of particle j, m is the particle mass, e is the restitution coefficient, and the asterisk (*) indicates a postcollision quantity.

Both binary and continuous particle size distributions (Gaussian and lognormal) are investigated. The preparation of continuous particle size distributions are detailed in [43]. Further details of the computational algorithm are available in [44], in which monodisperse systems were examined.

In the case of both binary and continuous size distribution systems, the restitution coefficient (e) and the concentration (area fraction) of the particle mixture in the system (ν) are dimensionless inputs. Further dimensionless parameters depend, however, on whether the system contains a binary or continuous size distribution. Binary systems are defined by two further dimensionless groups: the ratio of large- to small-particle diameters (d_L/d_S) and the area fraction of large particles relative to the total area fraction of the system (ν_L/ν). Systems containing continuous particle size distributions, on the other hand, are defined by one further dimensionless group: the coefficient of variation, i.e., the standard deviation of the particle size distribution normalized by the number average particle diameter (σ/d_{avg}). Investigated parameter ranges for binary systems are $\nu=0.2-0.4$, $e=0.6-0.8$, $d_L/d_S=1.0-2.5$, and $\nu_L/\nu=0.4-1.0$. For systems containing continuous size distributions, investigated parameter ranges are $\nu=0.2$, $e=0.6-0.8$, and $\sigma/d_{avg}=0.05-0.2$ for Gaussian, and $\sigma/d_{avg}=0.1-0.2$ for lognormal.

All system sizes have been chosen to allow for full development of clusters, as established for monodisperse systems by Liss *et al.* [13], i.e., the periodic domain size is large enough such that it does not limit the formation of clusters. Accordingly, binary systems are sized such that the ratio of the system size (L_{sys}) to the large-particle diameter (d_L) is 90. Likewise, continuous size distribution systems are sized such that the ratio of the system size to the root-mean-square diameter (d_{rms}) is 90. A common root-mean-square diameter has been chosen based on the work of Dahl *et al.* [43], in which d_{rms} was determined to be an appropriate characteristic diameter for the normalization of stresses in systems containing continuous size distributions. Given the common value of d_{rms} for the current continuous size distribution systems, "large" and "small" particles are defined as those greater than and less than d_{rms}, respectively. Consequently,

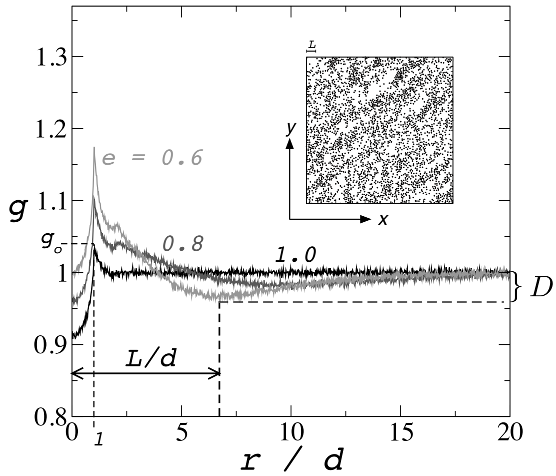

FIG. 1. (Color online) Radial distribution functions (g) for systems defined by $L_{sys}/d=110$, $\nu=0.2$, and $e=0.6$ (light gray), 0.8 (medium gray), and 1.0 (black). The r/d location of the long-scale minimum provides the normalized length scale (L/d) as indicated on plot for $e=0.6$. The value of L/d is also shown to scale by inset system snapshot for $e=0.6$.

continuous size distribution systems may be evaluated in a manner similar to systems containing a binary size distribution.

The MD outputs are targeted at cluster characterization and follow from the previous work on monodisperse systems [44]. Sections II A and II B contain further detail on the application of these cluster characterizations to polydisperse systems.

A. Radial distribution function for polydisperse systems

The radial distribution function (g) is a measure of the local particle density compared to the overall particle density, where local is defined as a given distance from the center of any particle. In the current work, distances are defined (nonconventionally) in a direction perpendicular to cluster alignment, as detailed in [44]. One further modification is made to the calculation of g in order to better reflect particle packing within polydisperse systems; local particle densities are evaluated on an area fraction basis, rather than the typical number basis, in order to account for the different size of particles and thus better reflect the mixture packing.

As first detailed in [44], a new feature arises in the radial distribution function of inelastic systems, namely a long-scale minimum. Figure 1 illustrates the appearance of this long-scale minimum for monodisperse simple shear flow systems as particles becomes more inelastic. The elastic system ($e=1.0$, black line) yields no long-scale minimum, while increased inelasticity (i.e., decreasing e) increases the prominence of this feature. The location of the long-scale minimum provides a length scale (L/d in Fig. 1, due to normalization by the particle diameter) associated with the distance between clustered and dilute regions. More specifically, this length scale is determined primarily by two physical attributes of the clustered system: the average distance from the center of a clustered region to the center of a dilute region in the direction perpendicular to cluster alignment, and the average width of the thinnest region (clustered or dilute). The connection between the length scale and these two physical attributes was established by the study of ideal one-dimensional systems [44]. More specifically, when clustered and dilute regions were patterned such that all clustered regions have equivalent widths and all dilute regions have equivalent widths, the length scale was determined by the width of the thinnest region (clustered or dilute). However, when clustered- and dilute-region widths were varied around a mean, the length scale tended toward the average distance from the center of a clustered region to the center of a dilute region. This latter scenario is expected to reflect the dynamic nature of two-dimensional simple shear flow systems examined here. In order to visualize this length scale, the inset of Fig. 1 illustrates the length scale L for $e=0.6$ alongside a corresponding system snapshot. For further discussion of the interpretation of the length scale, see [44] or [45].

In the case of polydisperse systems, the radial distribution function may be obtained separately for each species, as well as the mixture. As such, binary systems yield three length scales: L (mixture), L_L (large particles only), and L_S (small particles only). For systems containing continuous particle size distributions, three similar length scales are assessed, where large and small particles are defined relative to the d_{rms}, as discussed above.

B. Concentration and temperature measurements in clustered and dilute regions

Concentrations (area fractions) and temperatures associated with the clustered and dilute regions are measured as described in [44] for monodisperse systems, but a brief review of the methodology is provided here along with the natural extensions to polydisperse systems. As a first step, the discrete particle system is converted to a concentration grid, wherein the grid cells are approximately 20% of a reference particle size (d_L for binary distributions and d_{rms} for continuous distributions). Next, the grid is smoothed via a Gaussian filter, which is defined by its standard deviation ($\sigma_G=L/2$, with L obtained from the radial distribution function) and the number of standard deviations (four) that comprise the filter. After this smoothing of the concentration profile, each smoothed grid cell is designated as clustered or dilute depending on whether the cell concentration is above or below the average system value, respectively. Averaging of large-particle, small-particle, and mixture concentrations within the designated clustered and dilute regions then yields average region-specific concentrations of a particular particle type.

Following the calculation of average region-specific concentrations, cluster prominence is assessed based on normalized mixture concentration differences between the clustered and dilute regions: $(\nu_{clus}-\nu_{dil})/\nu$. A similar analysis of concentration differences may also be applied to individual species, in order to reveal segregation trends. Alternatively, species segregation trends can also be gleaned via comparison of the ratio of large- to small-particle concentrations in the two regions: $(\nu_L/\nu_S)_{clus}/(\nu_L/\nu_S)_{dil}$.

In the case of the temperature analysis, clustered and dilute regions are defined such that moderate concentrations, namely 15% above and below the average concentration, are excluded in order to better distinguish between the two regions. To determine the temperature, local bulk (average) velocities in the x direction (flow direction) are first found as a function of y by averaging the velocities of particles whose centers lie within bands of width L_g (grid cell size) at each y value. Average velocities in the y direction are assumed to be zero. Fluctuating velocities ($\vec{v}'$) may then be calculated for each particle in each snapshot as the difference between the actual particle velocity and the local bulk velocity. Granular temperatures (T) for the given instant may then be calculated with respect to each species (X) and each region (R, representing either the clustered or dilute region) via

$$T_{X,R} = \frac{1}{2}\frac{\sum_{i=1}^{N_{X,R}} m_i \vec{v}_i'^2}{N_{X,R}}, \quad (3)$$

where m represents the particle mass and $N_{X,R}$ represents the number of particles of species X in region R. Mixture temperatures for each snapshot are calculated via

$$T_R = \frac{N_{L,R}T_{L,R} + N_{S,R}T_{S,R}}{N_{L,R} + N_{S,R}}, \quad (4)$$

where subscripts L and S indicate the large and small-particle species, respectively. Ratios of clustered- to dilute-region temperatures are obtained based on these instantaneous temperature calculations, and final temperature ratios are determined by averaging the temperature ratios over all instants.

III. RESULTS AND DISCUSSION

The behavior of systems containing multiple particle sizes (i.e., binary and continuous size distributions) are investigated below. All data pertain to systems with a total particle concentration (ν) of 0.2. Binary data are shown for a restitution coefficient (e) of 0.6, and continuous size distribution data are shown for e=0.8. The higher restitution coefficient used for the continuous size distribution systems is necessary in order to avoid inelastic collapse [43,46]. Binary systems have also been considered for two higher total particle concentrations of ν=0.3 and 0.4 and a higher restitution coefficient of e=0.8. This broader parameter space reveals conclusions consistent with those discussed below, though a complete presentation of these additional data have not been shown here for the sake of brevity (see [45] for all data).

Binary data are generally presented as a function of diameter ratio (d_L/d_S) with each data set pertaining to a particular concentration of large particles relative to the overall particle concentration of the system (ν_L/ν). Data for systems containing continuous particle size distributions are presented as a function of the coefficient of variation, i.e., the standard deviation of the size distribution normalized by the mean of the distribution (σ/d_{avg}). Gaussian and lognormal distributions are studied. Error bars are shown for a subset of the data and indicate one standard deviation above and below the mean based on two duplicates.

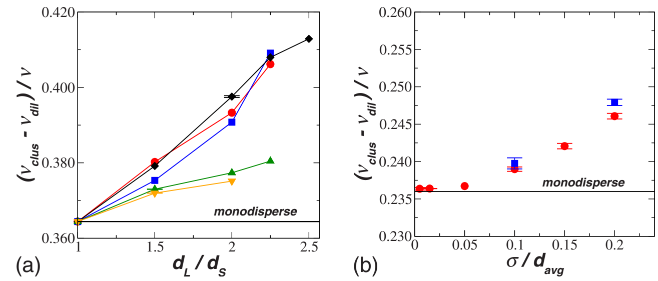

FIG. 2. (Color online) Normalized mixture concentration differences between the clustered and dilute regions. Horizontal lines indicate the monodisperse limits associated with the respective set of data. (a) Binary systems with ν=0.2 and e=0.6. Circles indicate ν_L/ν=0.40, squares indicate ν_L/ν=0.5, diamonds indicate ν_L/ν=0.57, upright triangles indicate ν_L/ν=0.9, and upside down triangles indicate ν_L/ν=0.95. (b) Continuous size distribution systems with ν=0.2 and e=0.8. Circles indicate Gaussian particle size distributions. Squares indicate lognormal particle size distributions.

Results presented below follow from the questions posed in the introduction. Section III A addresses the first question: Does the presence of size nonuniformities serve to enhance or attenuate the presence of clusters? Section III B addresses the second question: Do particles of a given size preferentially segregate within the clusters?

A. Cluster prominence

The question of whether multiple particle sizes serve to enhance or attenuate the presence of clusters in 2D simple shear flows may be observed by a measure of cluster prominence. For the purposes of the current work cluster, prominence is measured by the relative concentration (area fraction) in the clustered and dilute regions. Accordingly, normalized differences between the clustered- and dilute-region (mixture) concentrations are shown in Fig. 2. Binary mixture concentration differences are provided in subfigure (a) as a function of diameter ratio (d_L/d_S) for a variety of ν_L/ν values. Continuous size distribution data are provided in subfigure (b) as a function of the coefficient of variation (σ/d_{avg}) for both Gaussian and lognormal distributions. The monodisperse limit is indicated by the lower limit of the x axes shown, i.e., d_L/d_S=1 in subfigure (a) and σ/d_{avg}=0 in subfigure (b).

For binary systems [Fig. 2(a)], normalized concentration differences between clustered and dilute regions increase with increasing diameter ratio. This observation holds for all values of ν_L/ν tested, each of which is represented by a particular symbol on the plot. Similarly, for systems containing continuous particle size distributions [Fig. 2(b)], normalized concentration differences increase with an increased coefficient of variation. Both Gaussian and lognormal particle size distributions demonstrate this dependency. Therefore, regardless of the type of particle size distribution (i.e., binary, Gaussian, or lognormal), an increase in the particle size disparity leads to an increase in normalized concentration differences. In other words, the presence of increasingly disparate particle sizes serves to enhance the prominence of clusters (i.e., the clusters are more tightly packed with par-

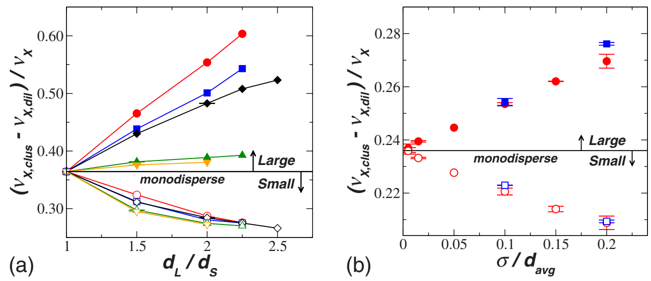

FIG. 3. (Color online) Species-specific concentration differences between the clustered and dilute regions for systems at $\nu=0.2$ and $e=0.6$. "X" refers to either the large (solid symbols) or small (open symbols) particles. Horizontal lines represent monodisperse concentration differences associated with the respective set of data. (a) Binary systems with $\nu=0.2$ and $e=0.6$. Circles indicate $\nu_L/\nu=0.40$, squares indicate $\nu_L/\nu=0.5$, diamonds indicate $\nu_L/\nu=0.57$, upright triangles indicate $\nu_L/\nu=0.9$, and upside down triangles indicate $\nu_L/\nu=0.95$. (b) Continuous size distribution systems with $\nu=0.2$ and $e=0.8$. Circles indicate Gaussian particle size distributions. Squares indicate lognormal particle size distributions.

ticles). This observation is distinct from, but complementary to that of Alam and Luding [24], who showed that the presence of a mass disparity in a binary (in size) mixture yields larger cluster sizes than the equivalent binary mixture in which the masses of the two species were equal. Combined, these two works indicate that clusters become larger and denser with size disparity.

B. Segregation

The question of species segregation between the transient clustered and dilute regions of a 2D simple shear flow may be addressed via a measure similar to that used for the assessment of cluster prominence. Normalized *species* concentration differences—$(\nu_{L,clus}-\nu_{L,dil})/\nu_L$ and $(\nu_{S,clus}-\nu_{S,dil})/\nu_S$—reflect the extent to which each species is distributed between the clustered and dilute regions. Increasing species concentration differences indicate that the species in question is becoming increasingly segregated toward the clustered regions, while decreasing species concentration differences indicate that the species in question is more homogeneously distributed between the clustered and dilute regions.

Figure 3(a) illustrates normalized species concentration differences for binary systems as a function of diameter ratio (d_L/d_S). Figure 3(b) illustrates normalized species concentration differences for continuous size distribution systems as a function of coefficient of variation (σ/d_{avg}). For both sets of data, solid and open symbols represent large and small particles, respectively.

Large-particle normalized concentration differences increase with size disparity in both the binary (subfigure a) and continuous size distributions (subfigure b). On the contrary, normalized concentration differences of small particles decrease with increasing size disparity. These trends reflect the tendency for large particles to become increasingly associated with clustered regions with increasing deviation from the monodisperse limit, while small particles become more homogeneously distributed throughout the system. Therefore, large particles do tend to segregate within clustered regions, and this tendency increases with increasing size disparity.

Having established the segregation of large particles within clustered regions, a follow-up question arises regarding the explanation for this segregation. Cattuto and Marconi [10] observed a similar form of segregation in a homogeneous cooling system containing two equally sized (different density) species. The observed segregation of the more massive species within the clustered regions was explained due to the level of nonequipartition (i.e., the extent to which the heavy-species temperature was greater than the light-species temperature) exhibited by the system. A theoretical level of nonequipartition was defined via a ratio of heavy- to light-species temperatures, above which the lighter species might be afforded greater mobility and consequent escape from clustered regions. While the systems in the current investigation exhibit a substantial nonequipartition of energy, they do not exhibit the level of nonequipartition deemed necessary for the mobility argument set forth by Cattuto and Marconi [10], as detailed in [45]. Moreover, the assumption of an equipartition of energy in a kinetic-theory-based study of species segregation in a system with a steady-state temperature gradient does not preclude species segregation [25]. Indeed, in the presence of a steady-state temperature gradient, the more massive particle species has been often observed to segregate toward the low-temperature regions [25,27–30]. Though two-dimensional simple shear flows do not exhibit steady-state temperature gradients, transient temperature gradients have been shown to exist across the surface of clusters in monodisperse systems [12,44]. To date, no observations of temperature gradients in clustering simple shear flows containing binary or continuous particle size distributions have been made. If these transient temperature gradients persist between clustered and dilute regions of polydisperse systems, the direction of the temperature gradient could provide an explanation for the observed segregation: Large particle may be driven toward the transient low-temperature clustered regions.

Employing the methodology discussed in Sec. II B, average (in time and space) temperatures of clustered and dilute regions may be obtained. The presence of temperature gradients between the clustered and dilute regions is assessed by ratios of clustered- to dilute-region temperatures (T_{clus}/T_{dil}) for the particle mixture. Temperature ratios below unity indicate that clustered regions exhibit lower temperatures than dilute regions. Figure 4 illustrates such temperature ratios for both binary (subfigure a) and continuous size distribution systems (subfigure b). Clustered regions consistently exhibit lower temperatures than dilute regions. Species-specific temperature ratios (not shown for the sake of space) exhibit similar temperature ratios (i.e., $T_{clus}/T_{dil}<1$). Therefore, the direction of the temperature gradient is consistent with the segregation patterns found in steady systems, namely large particles are driven toward the clustered (cooler) region.

Interestingly, in spite of increased segregation with increased size disparity [see Fig. 3(b)], an increase in size disparity yields a counterintuitive increase in the temperature ratio toward unity (Fig. 4), at which point no temperature-

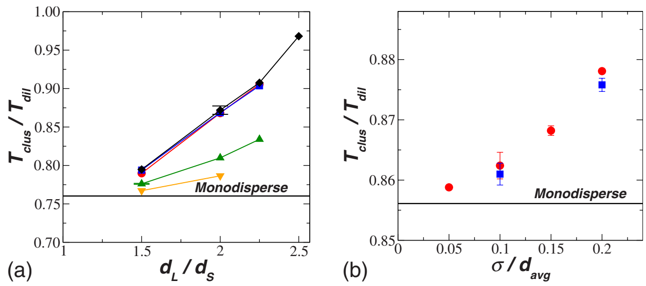

FIG. 4. (Color online) Ratios of clustered- to dilute-region temperatures. Horizontal lines indicate the monodisperse limits associated with the respective set of data. (a) Binary systems with $\nu=0.2$ and $e=0.6$. Circles indicate $\nu_L/\nu=0.4$, squares indicate $\nu_L/\nu=0.5$, diamonds indicate $\nu_L/\nu=0.57$, upright triangles indicate $\nu_L/\nu=0.9$, and upside down triangles indicate $\nu_L/\nu=0.95$. (b) Continuous size distribution systems with $\nu=0.2$ and $e=0.8$. Circles indicate Gaussian particle size distributions. Squares indicate log-normal particle size distributions.

based driving force would exist. Nevertheless, the temperature ratio itself is not a measure of the actual driving force (e.g., dT/dx), but rather its direction (i.e., the clustered regions are cooler than the dilute regions). Comparison of actual driving forces would be more desirable than the comparison of temperature ratios shown, but such calculations are nontrivial at best. The actual driving force, as it appears in kinetic theory, consists of a transport coefficient multiplied by the pertinent temperature gradient. The transport coefficients are functions of *local* volume fraction and temperature, as well as the diameter ratio. Moreover, assessment of the actual temperature gradient would require intimate knowledge of the temperature profile across the boundaries of the transient clusters. Appropriate averaging of these quantities would require elaborate averaging schemes, such as the spatial-temporal scheme utilized by Galvin *et al.* [29]. Unfortunately, the transient nature of the clusters in the current work would inhibit these schemes, which are more viable for systems with dense and dilute regions that are relatively stable in time and space (e.g., granular systems between two walls of different temperature, as in [29]). Clustered- and dilute-region characteristics for the current simple shear flow systems must be obtained by long-time system-wide averaging of continually moving and evolving clustered and dilute regions. Such averaging, as provided by the region temperature analysis, elucidates the low-temperature clusters, but not the explicit gradients across their boundaries. The pertinent observation is that the *direction* of the temperature gradients across the cluster interface is consistent with that expected to drive large particles toward clustered regions.

Length scales obtained from the radial distribution function provide further insight into species segregation trends, namely that related to species segregation *within* a cluster (whereas the previous data shed light only on segregation tendencies *between* clustered and dilute regions). This insight is based on an interesting difference between the length scales for a given system. Figure 5 reveals this difference for binary systems with $\nu=0.2$, $e=0.6$, and $d_L/d_S=1.5$ over a range of ν_L/ν. Monodisperse limits are represented by horizontal lines indicating length scales for systems containing small ($\nu_L/\nu=0$) or large ($\nu_L/\nu=1$) particles only. Large-particle, small-particle, and mixture length scales all follow a trend with increasing ν_L/ν consistent with the connection (across ν_L/ν) between the monodisperse limits. However, the key observation is the relationship between the three length scales at a given value of ν_L/ν, which may be summarized as $L_S>L>L_L$. The forthcoming discussion provides a physically plausible explanation for this length scale observations that is consistent with the temperature-driven segregation described above. The stage for this explanation will first be set by using an idealized system to demonstrate a supposed, yet reasonable, relationship between species length scales and species spatial distribution. Length scales for binary and continuous size distributions will then be discussed accordingly.

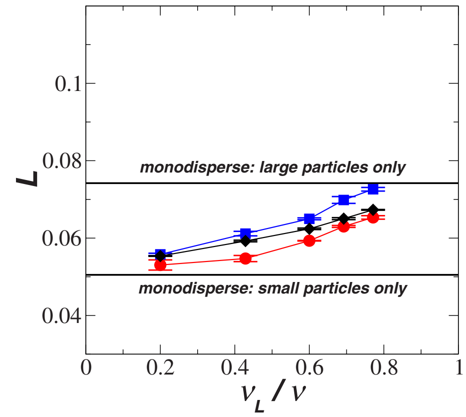

FIG. 5. (Color online) Length scales for binary systems with $\nu=0.2$, $e=0.6$, and $d_L/d_S=1.5$. Length scales are provided for the mixture (diamonds), large particles only (circles), and small particles only (squares). The horizontal line indicates the monodisperse reference value associated with a system containing large particles only and small particles only, as labeled.

Consider first the ideal representation of clustered and dilute regions shown in Fig. 6. The system contains two species, A and B. Shaded ellipsoidal regions represent the clustered regions, in which the concentration of each species will be greater than the respective species concentration in the dilute regions (spaces between the ellipsoids). Species B is (approximately) homogeneously distributed throughout the clustered regions, while species A exhibits preferential segregation toward the center of the clustered regions (dark shading) and decreasing concentration toward the cluster surface (light shading).

Application of the radial distribution function to such a polydisperse system will assess each species independently of other species. Consequently, the length scales resulting from the analysis of a particular species will reflect physical properties (e.g., different clustered- and dilute-region widths) pertaining only to the distribution of that species. In the case presented in Fig. 6, the preferential segregation of species A toward the center of the clustered regions would cause the analysis of species A to perceive clusters as "thin" (cluster center only). On the contrary, the analysis of species B would perceive clusters as "thick" (cluster center and surface region). Accordingly, the analysis of the mixture would per-

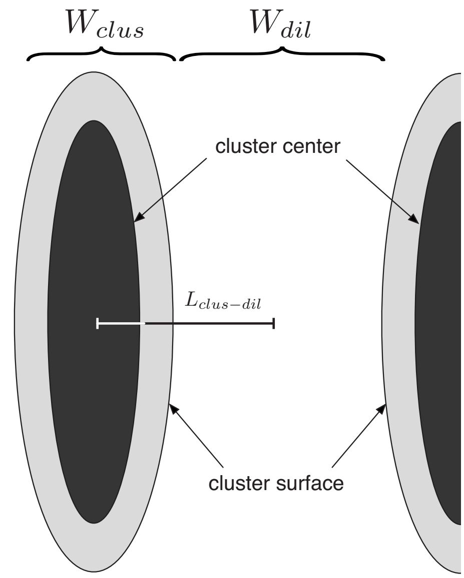

FIG. 6. Ideal representation of clustered and dilute regions. The region of darkest shading represents the center of the cluster, while the region of lighter shading represents the cluster surface. The distance from the center of the clustered region to the center of the dilute region is represented by the line labeled as $L_{clus\text{–}dil}$.

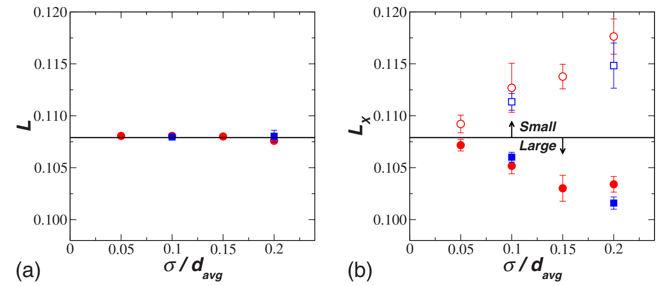

FIG. 7. (Color online) Length scales for systems with ν=0.2, e=0.8, and continuous particle size distributions. Circles indicate Gaussian particle size distributions. Squares indicate lognormal particle size distributions. The horizontal lines indicates the monodisperse reference value associated with a system in which d=d_{rms}, ν=0.2, and e=0.8. (a) Mixture length scales. (b) Large- and small-particle length scales, where X indicates the species. Closed symbols represent large particles. Open symbols represent small particles.

ceive cluster widths between those of species A and B.

Recall from Sec. II A that the length scale value is affected by two physical properties: the average distance from the center of a clustered region to the center of a dilute region ($L_{clus\text{–}dil}$) and the average width of the thinnest region (W_{clus} or W_{dil}). For systems in which clustered and dilute regions vary about a mean, the value of $L_{clus\text{–}dil}$ is expected to be dominant. Since Fig. 6 represents averaged clustered and dilute regions (i.e., cluster and dilute-region widths vary around those shown), the length scale values for both species (and the mixture) will tend toward $L_{clus\text{–}dil}$. Small differences between the species length scales will arise due to the impact of the thinnest region, which is the clustered region in the case of both species. Deviation from $L_{clus\text{–}dil}$ will occur toward the width of the thinnest region, i.e., length scales associated with each species (L_A and L_B) will decrease relative to the average width of the clustered regions perceived by the respective species. Since clustered regions are perceived to be thinner for species A compared to species B, L_A is expected to deviate from $L_{clus\text{–}dil}$ more than L_B, yielding length scales that could be summarized as $L_B > L_A$. Moreover, the mixture length scale (L) will naturally tend to lie between the two species length scales.

This $L_B > L > L_A$ relationship for the idealized system is consistent with that exhibited by binary systems (Fig. 5), for which $L_S > L > L_L$. The similarity suggests that large particles may tend toward the center of the clustered regions, expanding upon the segregation observations offered earlier by Fig. 3. More specifically, whereas the previous concentration data indicated species segregation *between* clustered and dilute regions, species length scales offer added insight regarding species segregation *within* the clustered regions.

Further substantiation of the similarity between the ideal scenario (Fig. 6) and binary systems is provided by the consideration of two points. First, via the concentration analysis, which assesses clustered and dilute regions based on the mixture concentration, both species may be shown to exhibit higher concentrations in the clustered regions than in the dilute regions. This observation suggests that both species are present in the same clusters (rather than each species forming separate clusters dominated by only one species; this behavior is confirmed by visual analysis of snapshots as well), implying that clustered-region centers are the same from the perspective of both species. Second, clustered regions are reasonably considered to be thinner than dilute regions for this region of the parameter space; the low total particle concentration (ν=0.2) suggests that the overall system will not be tightly packed with particles, while the low restitution coefficient (e=0.6) is likely to result in more tightly packed clusters. Consequently, the similarity of this physical picture with that of Fig. 6 suggests that large particles may not only tend toward the low-temperature clustered regions (Fig. 3), but also toward the center of the cluster itself. Since the center of the clustered region will exhibit an increased collision rate and consequent energy dissipation, a minimum in temperature is expected at this point. Therefore, the segregation of large particles toward the *center* of the clustered regions is consistent with the segregation of large particles toward low-temperature regions.

Having established a plausible physical picture of intracluster species segregation within binary systems, length scale data for systems containing continuous particle size distributions are shown in Fig. 7 for systems with ν=0.2 and e=0.8. Mixture (subfigure a) and species (subfigure b) length scales for systems containing Gaussian and lognormal particle size distributions are shown as functions of σ / d_{avg}. The horizontal lines indicate the monodisperse reference value for a system in which d is the root-mean-square diameter (i.e., the diameter that is consistent among all continuous size distribution systems). Mixture length scales [Fig. 7(a)] exhibit little deviation from the monodisperse reference value, regardless of the particle size distribution. Such consistency in the mixture length scale suggests that average widths of the clustered and dilute regions change little with the width of the particle size distribution.

Species length scales demonstrate more change as a function of σ/d_{avg}, as illustrated in Fig. 7(b). Within the constraints of the error shown, deviation of both large- and small-particle length scales from the monodisperse reference value appears to increase with an increasing width of the particle size distribution (σ/d_{avg}). Furthermore, large- and small-particle length scales deviate from the monodisperse reference value in opposite directions: the small-particle length scales are greater, while the large-particle length scales are less. Therefore, the physical picture painted for large and small particles of binary systems at $\nu=0.2$ and $e=0.6$ applies to the systems of continuous particle size distributions studied here. Namely, the large particles may tend toward the center of the low-temperature, clustered regions, where the temperature is expected to reach a minimum.

As a final note, the consistency of these species length scale trends should be briefly discussed. While cluster prominence and species segregation trends are consistent across the broader parameter space not shown here (i.e., higher total particle concentrations and restitution coefficients noted at the beginning of Sec. III), the relationship between species length scales is not consistent across this parameter space. However, the relationship between species length scales may be consistently explained by the segregation of large particles toward the center of the clustered regions. Detailed discussion of this broad parameter space is reserved for the thesis in [45].

IV. CONCLUSIONS

The dynamic clusters arising from instabilities in two-dimensional simple shear flows have been investigated for systems containing mixtures of equal-material-density particles. Binary size distributions have been studied for a range of total particle concentrations, restitution coefficients, diameter ratios, and relative fractions of each species, though the presented data has been limited to an illustrative subset of data at $\nu=0.2$ and $e=0.6$. Continuous size distributions have been studied for a range of Gaussian and lognormal size distributions at $\nu=0.2$ and $e=0.8$. An analysis of clustered- and dilute-region concentrations has been employed in combination with the radial distribution function in order to elucidate the answers to two questions: Does the presence of size nonuniformities serve to enhance or attenuate the presence of clusters? Do particles of a given size preferentially segregate within the clusters?

Throughout the investigated parameter space, including binary, Gaussian, and lognormal particle size distributions, the answers to the above questions are consistent. The answer to the first question is assessed by defining the cluster prominence as the normalized difference between clustered- and dilute-region concentrations $[(\nu_{clus}-\nu_{dil})/\nu]$. Clusters are consistently observed to become more prominent (tightly packed) with increasing deviation from the monodisperse limit (i.e., increasing diameter ratio or increasing size distribution width). The answer to the second question is found in a similar manner using species-specific concentration differences. Specifically, large particles consistently segregate toward the clustered regions. Further analysis of clustered and dilute-region temperatures in these polydisperse systems reveals that clusters exhibit lower temperatures than surrounding dilute regions. Consequently, the observed species segregation is consistent with temperature-driven segregation of the more massive particles toward low-temperature regions. While temperature-driven segregation has previously been observed for systems exhibiting *steady-state* temperature gradients, the current work demonstrates the potential for such segregation in the context of the *transient* temperature gradients associated with the dynamic clusters of 2D simple shear flow. Moreover, a plausible explanation for the behavior of species-specific clustering length scales obtained from the radial distribution function corroborates the possibility of temperature-driven segregation by suggesting that large particles may favor the center of the clustered regions (i.e., segregation *within* clustered regions), where granular temperatures are expected to reach a minimum. Accordingly, an important finding of the current effort is the presence of species segregation in dynamic systems, in which the dominant driving forces for segregation appear consistent with those in steady systems, thereby implying that the time needed for steady-state diffusion to occur is less than the lifetime of the cluster itself. Confirmation of the proposed segregation explanation is possible via a solution of the *transient* form of the kinetic-theory-based description for mixtures (see, for example [47,48], and works reviewed within). In granular flows, such transient solutions have been applied to a monodisperse homogeneous cooling system [49], though an extension to polydisperse systems is expected to increase computational requirement considerably.

Furthered understanding of the role of multiple species in the dynamic clusters of granular systems (i.e., those studied in the current work) could provide insight into the well-documented dynamic clusters observed in gas-solid systems. In particular, this insight could shed light on the peculiar role of fines [50,51] in the flow characteristics of fluidized beds (e.g., fluidized catalytic cracking units), wherein both hydrodynamic and granular effects will affect the prominence and nature (e.g., the presence of species segregation) of the clustered regions.

ACKNOWLEDGMENTS

The authors are grateful to the American Chemical Society Petroleum Research Fund (Grant No. ACS PRF 38065-AC9) and the U.S. Department of Energy (Grant No. DE-FC26-07NT43098) for the funding to support this work. R.B.R. also acknowledges support provided by the Department of Education (Grant No. P200A980454).

[1] *Statics and Kinematics of Granular Materials*, edited by R. M. Nedderman (Cambridge University Press, Cambridge, 1992).
[2] C. S. Campbell, Annu. Rev. Fluid Mech. **22**, 57 (1990).
[3] H. M. Jaeger, S. R. Nagel, and R. P. Behringer, Rev. Mod. Phys. **68**, 1259 (1996).
[4] L. P. Kadanoff, Rev. Mod. Phys. **71**, 435 (1999).
[5] R. Behringer, H. Jaeger, and S. Nagel, Chaos **9**, 509 (1999).
[6] I. Goldhirsch, Annu. Rev. Fluid Mech. **35**, 267 (2003).
[7] T. M. Knowlton, J. W. Carson, G. E. Klinzing, and W. C. Yang, Chem. Eng. Prog. **90**, 44 (1994).
[8] M. A. Hopkins and M. Y. Louge, Phys. Fluids A **3**, 47 (1991).
[9] I. Goldhirsch and G. Zanetti, Phys. Rev. Lett. **70**, 1619 (1993).
[10] C. Cattuto and U. M. Marconi, Phys. Rev. Lett. **92**, 174502 (2004).
[11] T. Pöschel, N. V. Brilliantov, and T. Schwager, J. Phys.: Condens. Matter **17**, S2705 (2005).
[12] M. L. Tan and I. Goldhirsch, Phys. Fluids **9**, 856 (1997).
[13] E. D. Liss and B. J. Glasser, Powder Technol. **116**, 116 (2001).
[14] M. E. Lasinski, J. S. Curtis, and J. F. Pekny, Phys. Fluids **16**, 265 (2004).
[15] S. L. Conway, X. Liu, and B. J. Glasser, Chem. Eng. Sci. **61**, 6404 (2006).
[16] S. L. Conway and B. J. Glasser, Phys. Fluids **16**, 509 (2004).
[17] *Granular Gases*, edited by T. Pöschel and S. Luding (Springer, New York, 2000).
[18] F. Spahn, J. Schmidt, O. Petzschmann, and H. Salo, Icarus **145**, 657 (2000).
[19] P. Tanga, S. J. Weidenschilling, P. Michel, and D. C. Richardson, Astron. Astrophys. **427**, 1105 (2004).
[20] *Multiphase Flow and Fluidization: Continuum and Kinetic Theory Descriptions*, edited by D. Gidaspow (Academic, New York, 1994).
[21] *Principles of Gas-Solid Flows*, edited by L. S. Fan and C. Zhu (Cambridge University Press, Cambridge, 1998).
[22] K. Agrawal, P. N. Loezos, M. Syamlal, and S. Sundaresan, J. Fluid Mech. **445**, 151 (2001).
[23] M. E. Möbius, Phys. Rev. E **74**, 051304 (2006).
[24] M. Alam and S. Luding, Phys. Fluids **17**, 063303 (2005).
[25] S. S. Hsiau and M. L. Hunt, Acta Mech. **114**, 121 (1996).
[26] J. T. Jenkins and F. Mancini, Phys. Fluids A **1**, 2050 (1989).
[27] S. Luding, O. Strauss, and S. McNamara, in *Symposium on Segregation in Granular Flows*, edited by A. D. Rosato and D. L. Blackmore, IUTAM (Kluwer Academic, Boston, 2000), pp. 297–303.
[28] B. O. Arnarson and J. T. Jenkins, Phys. Fluids **16**, 4543 (2004).
[29] J. E. Galvin, S. R. Dahl, and C. M. Hrenya, J. Fluid Mech. **528**, 207 (2005).
[30] S. R. Dahl and C. M. Hrenya, Phys. Fluids **16**, 1 (2004).
[31] J. M. Ottino and D. V. Khakhar, Annu. Rev. Fluid Mech. **32**, 55 (2000).
[32] J. T. Jenkins, *Physics of Dry Granular Media* (Kluwer Academic, Boston, 1998), p. 645.
[33] D. V. Khakhar, J. J. McCarthy, and J. M. Ottino, Chaos **9**, 594 (1999).
[34] B. O. Arnarson and J. T. Jenkins, *Traffic and Granular Flow '99: Social, Traffic, and Granular Dynamics* (Springer, Berlin, 2000).
[35] M. Schröter, S. Ulrich, J. Kreft, J. B. Swift, and H. L. Swinney, Phys. Rev. E **74**, 011307 (2006).
[36] J. T. Jenkins and D. K. Yoon, Phys. Rev. Lett. **88**, 194301 (2002).
[37] J. J. Brey, M. J. Ruiz-Montero, F. Moreno, Phys. Rev. Lett. **95**, 098001 (2005).
[38] D. Serero, I. Goldhirsch, S. Noskowicz, and M.-L. Tan, J. Fluid Mech. **554**, 237 (2006).
[39] R. D. Wildman, J. T. Jenkins, P. E. Krouskop, and J. Talbot, Phys. Fluids **18**, 073301 (2006).
[40] X. Liu, M. Metzger, and B. J. Glasser, Phys. Fluids **19**, 073301 (2007).
[41] V. Garzó, Eur. Phys. J. E **29**, 261 (2009).
[42] *Computer Simulation of Liquids*, edited by M. P. Allen and D. J. Tildesley (Oxford University Press, New York, 1989).
[43] S. R. Dahl, R. Clelland, and C. M. Hrenya, Phys. Fluids **14**, 1972 (2002).
[44] R. B. Rice and C. M. Hrenya, Phys. Rev. E **79**, 021304 (2009).
[45] R. B. Rice, Ph.D. thesis, University of Colorado at Boulder, 2009.
[46] M. Alam and C. M. Hrenya, Phys. Rev. E **63**, 061308 (2001).
[47] V. Garzó, J. W. Dufty, and C. M. Hrenya, Phys. Rev. E **76**, 031303 (2007).
[48] V. Garzó, C. M. Hrenya, and J. W. Dufty, Phys. Rev. E **76**, 031304 (2007).
[49] N. Brilliantov, C. Saluena, T. Schwager, and T. Pöschel, Phys. Rev. Lett. **93**, 134301 (2004).
[50] J. M. Matsen, in *Circulating Fluidized Beds*, edited by J. R. Grace, A. A. Avidan, and T. M. Knowlton (Chapman & Hall, London, 1997).
[51] J. Choi, J. Suh, I. Chang, D. Shun, C. Yi, J. Son, and S. Kim, Powder Technol. **121**, 190 (2001).